Analytical Biochemistry 428 (2012) 119–125

Contents lists available at SciVerse ScienceDirect

Analytical Biochemistry

journal homepage: www.elsevier.com/locate/yabio

Detection of hepatitis B surface antigen by target-induced aggregation monitored by dynamic light scattering

Xiaohui Wang [a,1], Yuan Li [a,1], Dongqin Quan [b], Jidong Wang [a], Yuhua Zhang [a], Juan Du [a], Jianchun Peng [a], Qiuxia Fu [a], Yong Zhou [a], Shuaizheng Jia [a], Yingli Wang [a], Linsheng Zhan [a,*]

[a] Beijing Institute of Transfusion Medicine, Beijing 100850, People's Republic of China
[b] Beijing Institute of Pharmacology and Toxicology, Beijing 100850, People's Republic of China

ARTICLE INFO

Article history:
Received 18 March 2012
Received in revised form 11 June 2012
Accepted 12 June 2012
Available online 20 June 2012

Keywords:
Dynamic light scattering
Gold nanoparticles
Detection
HBsAg

ABSTRACT

In the current work, a one-step, washing-free, homogeneous nanosensor assay has been constructed to sensitively detect hepatitis B surface antigen (HBsAg) based on the light scattering property of gold nanoparticles (GNPs) through a sandwich model. The two nanoprobes in this study were designed by conjugating monoclonal and polyclonal hepatitis B surface antibody (HBsAb) onto the GNPs of different diameters. First, the detection behavior of the combinations of different sizes of GNPs was evaluated and the optimized combination was determined. In analyzing HBsAg in Tris–HCl buffer, such bioassay composed of GNPs of approximately 50 and 100 nm has a limit of detection (LOD) as high as 0.005 IU/ml and a dose-dependent response ranging from 0.005 to 1 IU/ml, which indicates its good diagnostic capability and provides a useful means to analyze protein biomarkers with low virus loads. Observation with transmission electron microscopy (TEM) provides direct evidence that the increase of hydrodynamic diameters resulted from the aggregation induced by immunological reactions. The bioassay also exhibits satisfactory specificity in analyzing HBsAg in serum media. Therefore, with its simple preparation, easy readout, and good stability, this bioassay has the potential to be developed into an automated and widely used biosensor assay.

Gold nanoparticles (GNPs)[2] are currently used for a growing number of applications because of their unique optical properties, including biomedical diagnostics [1–8], molecular and cell imaging [9–11], and thermal ablation and radiotherapy [12–15]. Nanoparticles exist in the same size domain of protein and DNA structure, which allows researchers to apply them as biomarkers in tagging or labeling in diagnostics. The GNPs modified by a biological coating or layer construct the nanosensors or nanoprobes. The principle underlying the assay is based on GNPs' ability to convert signals of interactions between probe molecules and targets into easily monitoring optical signals, such as colorimetric detection [16–18], surface plasmon resonance (SPR) [2,3,19,20], and fluorescent quenching and enhancement [21–23].

Among them, colorimetric detection provides a simple, cheap, and portable way of detecting the protein and DNA of interest. Especially, gold colloid-based lateral flow immunoassay has been widely used as an effective field diagnosis method and point-of-care technology. The aggregation and network formation generated by biological reactions results in color change, which constitutes the basis of colorimetric detection methods. However, the limit of detection (LOD) of these bioassays can hardly be upgraded due to the absence of amplification except for some exploration studies in bio-barcode assays with fine design [24–29]. Whereas the SPR property-based bioassays are nearly sensitive enough, such a nanoprobe is particular about the external environment for the homogeneous assays. Moreover, the preparation of solid SPR nanoprobe chips needs multiple steps for the heterogeneous ones [30]. Besides, fluorescent technology has been studied extensively due to its high sensitivity, broad dynamic range, and multiplexing capabilities. However, the fluorophores often blink or bleach, which affects their signal collections and observations and limits its wide applications.

The dynamic light scattering (DLS) technique is routinely used as a conventional method to measure the hydrodynamic size and size distribution of nanoparticles. Since the 1970s, it has been employed as an analysis method for immunological diagnosis [31]. Recently, a homogeneous DLS-based bioassay was reported to exhibit superior performance on the detection of protein and DNA

* Corresponding author. Fax: +86 10 66931292.
E-mail address: lszhan91@yahoo.com (L. Zhan).

[1] These authors contributed equally to this work.

[2] *Abbreviations used:* GNP, gold nanoparticle; SPR, surface plasmon resonance; LOD, limit of detection; DLS, dynamic light scattering; HBV, hepatitis B virus; HBsAg, hepatitis B surface antigen; ELISA, enzyme-linked immunosorbent assay; BSA, bovine serum albumin; HBsAb, hepatitis B surface antibody; HCV, hepatitis C virus; OD, optical density; TEM, transmission electron microscopy; UV–Vis, ultraviolet–visible.

0003-2697/$ - see front matter © 2012 Elsevier Inc. All rights reserved.
http://dx.doi.org/10.1016/j.ab.2012.06.011

targets [32–36]. Actually, the previous studies offered great promise that optical cross sections of gold-based nanomaterials are orders of magnitude higher than those of the conventional fluorescing dyes, polystyrene nanospheres, or quantum dots [37]. Therefore, it stands to reason to use gold nanomaterials as the light scattering enhancer, which would allow researchers to examine the microscopic changes of the dispersion state caused by interactions between the probes labeled.

Here, we report an ultrasensitive, one-step, homogeneous GNP probe-based immunoassay to detect the target protein through a sandwich assay format. Two possible sensing combinations were evaluated, and a more appropriate one is demonstrated. As a proof-of-concept example, the most important marker for the laboratory diagnosis of hepatitis B virus (HBV), namely hepatitis B surface antigen (HBsAg), was chosen as a target. HBsAg indicates potential infectivity of HBV, and its quantity detection may be contributed to the follow-up of treatment of HBV with antiviral drugs. In general, it is qualitatively detected by enzyme-linked immunosorbent assay (ELISA) and quantitatively analyzed through chemiluminescence detection clinically. Thus, our approach not only provides a novel method of ultrasensitive detection of HBV, even in serum, but also overcomes some of the drawbacks of ELISA, such as the long testing time and the multiple washing steps.

Materials and methods

Materials

Chloroauric acid and citrate sodium were purchased from Sigma–Aldrich Chemical. Bovine serum albumin (BSA) was purchased from Roche. Monoclonal and polyclonal hepatitis B surface antibody (HBsAb) and HBsAg were provided by Beijing Polaris Biotechnology. The HBV, hepatitis C virus (HCV), and syphilis-positive sera were obtained from the commercial diagnostic kits of InTec Products (Xiamen, China), in which positive controls are the purified serum spiked with the antigen protein. The standard reference material for HBsAg was provided by the National Center of Clinical Laboratory (NCCL) of China. In addition, all of the chemical reagents were of analytical grade, and ultrapure water with a minimum resistance of 18.2 $M\Omega\,cm^{-1}$ produced by a Milli-Q system was used in all experiments.

Apparatus

Absorption spectra of the GNPs and GNP-based probes were recorded with a SpectraMax M5 microtiter plate reader with SoftMax Pro software (Molecular Devices) in the wavelength range of 400 to 700 nm. The size measurements were carried out on a Zetasizer Nano ZS90 system (Malvern Instruments) at a scattering angle of 173°. All of the data were obtained after being averaged from three parallel experiments and expressed as means ± standard deviations. A Hitachi H-7650 transmission electron microscope operating at 80 kV was used to observe the morphology of GNP-based probes.

Preparation of GNPs with different radius

The GNPs of different sizes were synthesized by the reduction of chloroauric acid by citrate sodium according to a method described elsewhere [38,39]. The dosage of the reducing agent was determined as we had done before [40]. All glassware was treated by silylation due to the enhancement of the surface hydrophobicity. As the first step, 250 μl of the 4 wt.% $HAuCl_4$ aqueous solution was added to 100 ml of water in a flask under stirring at room temperature. Then, the system was heated to 130 °C in an oil bath. After that, different volumes of 1 wt.% citrate sodium solution were quickly added to the flask to obtain GNPs with different sizes. Thereafter, the significant color change of the solution was observed at once. After being boiled for at least 15 min, the reaction system was removed from the oil bath and cooled at room temperature. Prior to use, no purification procedure was needed for the as-prepared GNPs. For convenience, we denoted the GNPs with diameters of approximately 10, 50, and 100 nm as GNP10, GNP50, and GNP100, respectively.

Surface modification of GNPs

The monoclonal and polyclonal HBsAbs were bound onto the GNPs by the general conjugation protocol through physical adsorption. For the purpose of sensing model evaluation, the GNP50s were labeled by monoclonal antibodies, and the GNP10s and GNP100s were labeled by polyclonal antibodies, which allowed us to compare the sensing behavior of the combination of GNP10–GNP50 and GNP100–GNP50 to detect HBsAg through the sandwich model. Prior to conjugation, the pH value of the GNP colloidal solution had been adjusted by 0.1 M K_2CO_3 according to the isoelectric point of the antibodies. The concentration of antibodies had been determined by the salt-induced aggregation observations. The optimized protein concentrations were 54 and 108 μg/ml polyclonal HBsAb onto GNP10 and GNP100, respectively, and 120 μg/ml monoclonal HBsAb onto GNP50. To be more detailed, the optimized amounts of the antibodies were added to the colloidal gold with gentle shaking, followed by remaining motionless for an incubation period of 30 min. Then, the GNP–antibody conjugates were washed by Tris–HCl buffer (pH 7.4) containing 1 wt.% BSA three times by centrifugation to block the active sites that remained on the GNPs.

In vitro detection of HBsAg through sandwich format

First, the nanoprobes were condensed by adjusting their light absorption values to an optical density (OD) of 0.8, monitored through the particle surface plasmon resonance. The two sorts of nanoprobes were mixed with a certain volume ratio in the 10 mM Tris–HCl buffer (pH 7.4). Once prepared, simulated target samples were added into the mixture immediately, and a 1-h incubation at 37 °C was carried out. Then, the DLS measurements were directly performed within 1 h. Each value was averaged from three parallel experiments and expressed as mean ± standard deviation. If transmission electron microscopy (TEM) observations were conducted, the reaction products should be collected by centrifugation because the concentrations of the nanoparticles were too low for TEM.

Results and discussion

Characterization and fabrication of nanoprobes

It is well known that GNPs exhibit a localized SPR property that is manifested by an absorption band in the visible region of the optical spectrum. As shown in Fig. 1, the SPR peaks of the three sorts of nanoparticles were located at 524, 540, and 565 nm, in good agreement with the published data [40]. The core sizes of the GNPs were determined by TEM analysis (insets of Fig. 1), and the average core diameters of GNP10s, GNP50s, and GNP100s were approximately 12.6 ± 1.0, 53.7 ± 5.9, and 93.6 ± 16.8 nm, respectively. As has been applied elsewhere, the nanoprobes were fabricated through physical adsorption with the system pH value at, or a litter higher than, the p*I* value of the antibodies to allow the most proteins to be adsorbed onto the surface of GNPs and to obtain

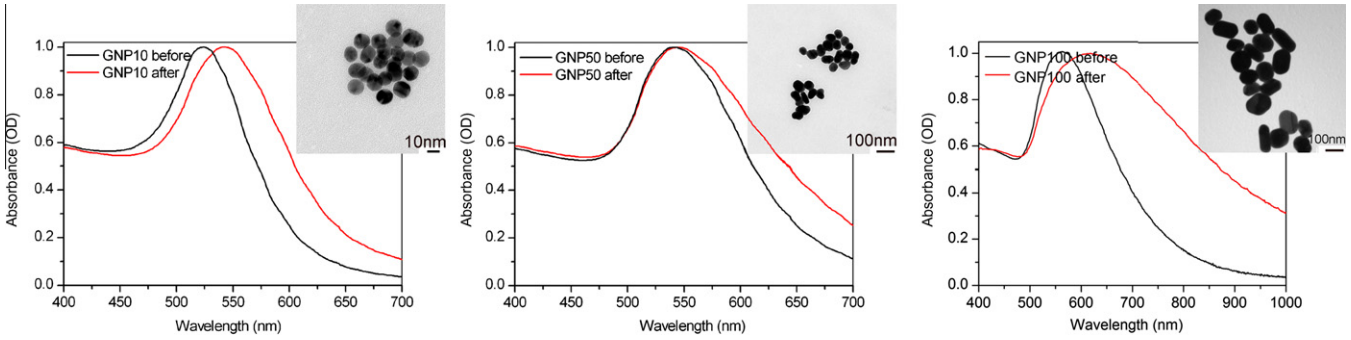

Fig.1. Normalized UV–Vis absorption spectrum of the GNPs before and after the antibodies were modified. The insets are the TEM micrographs of the as-prepared GNPs.

stable detection systems. As shown in Fig. 1, functionalization by antibodies brought about some changes to the location or shape of the absorption spectroscopy.

Schematic illumination

Fig. 2 presents the schematic illumination of the two nanoprobes in detecting the corresponding target based on the DLS technique. The combination of GNP10–GNP50 was taken, for example, in the figure. Nanoprobes were formed after antibodies are conjugated onto the GNPs, and the stability of the colloid solution was increased compared with the unbound metal colloidal solutions. HBsAg was chosen as the analyte because of its significance in clinical diagnosis. The target, once added, would act as the bridge to link the antibody-labeled GNP10 and GNP50 owing to the immunological reactions through the sandwich model, just as illuminated in Fig. 2Ba and 2Bc. Meanwhile, it is worth noting that the aggregates would probably exist as another different form in the detection system, as shown in Fig. 2Bb. Considering the polyclonal nature of GNP10s, the presence of target resulted in the aggregation between the GNP10s because it allowed multiple binding to the many paratopes that existed on the target antigen. As a result, the nanoparticles' aggregation could be detected directly by measuring their changes in hydrodynamic size rather than by observing the color change with the naked eye or through the ultraviolet–visible (UV–Vis) absorption spectroscopy. Huo and coworkers verified that the nanoparticles' pairs and oligomers were formed from binding between the antigen and the primary

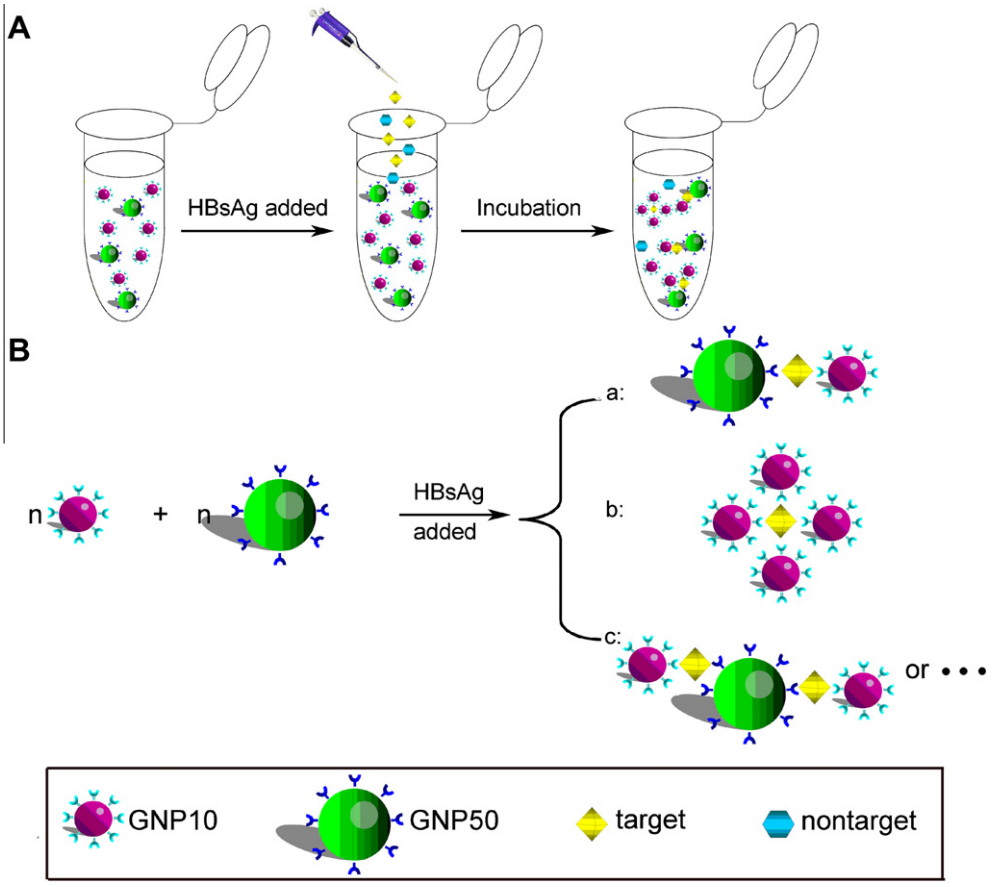

Fig.2. Schematic illumination of the two nanoprobes in diagnostics using the DLS technique. (A) Dispersion state of the mixed nanoprobes in the detection system. (B) Possible aggregates formed as a result of antigen–antibody reactions in the presence of target.

antibodies attached to nanoprobes by adding a secondary antibody and observation by TEM [36].

Model evaluation and detecting HBsAg in Tris–HCl buffer

The concentrations of the nanoprobes are conventionally adjusted to the appropriate ones for DLS analysis because it has been demonstrated to be critical for the performance of the assay [41], which could be easily monitored by the UV–Vis measurements. By adjusting the light absorption intensity to OD = 0.8, the molar concentrations of the nanoprobes were calculated to be approximately 3.13 nM (GNP10), 0.03 nM (GNP50), and 6.42 pM (GNP100) according to the molar extinction coefficients at 450 nm [42]. The polyclonal antibody-labeled GNP10s were mixed with monoclonal antibody-labeled GNP50 nanoprobes in a 1:3 volume ratio to construct the detection system. For comparison purposes, the antibody-labeled GNP100s were also mixed with GNP50 in the same volume ratio. To make the data obtained from the current work more comparable with those of other studies, HBsAg standard material was used as an analyte in the as-prepared biosensor assay due to its stability. The diagnostic behavior of the combinations of GNP10–GNP50 and GNP100–GNP50 toward the concentration of HBsAg ranging from 0.001 to 1 IU/ml was investigated and is plotted in Figs. 3 and 4. Inspection of the data showed that the *Z*-average diameters of the detection systems increased in a dependent manner with the amount of target protein in both figures, which verified the principle described above. The LODs were determined to be 0.01 and 0.005 IU/ml for GNP10–GNP50 and GNP100–GNP50, respectively, which corresponded to the signals that were greater than 3 times the standard deviation of the blank samples. In comparison with the combination of GNP10–GNP50, it is obvious that the combination of GNP100–GNP50 exhibited good performance in terms of high sensitivity and broad dynamic range. This is because the scattering light intensity of GNP100s was much stronger than that of GNP10s with the same quantity. So, despite the fact that GNP10s were numerically superior to GNP100s, the combination of GNP100–GNP50 was demonstrated to be more suitable than that of GNP10–GNP50 in the current detection system. Actually, the aggregation caused by antigen–antibody reaction increased the average particle size by several times, which has also been observed in published works [41,43]. This phenomenon might be attributed to the fact that for the current assay, dimers, trimers, or clusters would occur as immunological reaction-induced products, as illuminated in Fig. 2. However, because of the increased electrostatic or steric repulsion, the aggregates were not large enough to change the solubility of the whole detection system, which allowed the observations by DLS. As shown, the mixed nanoprobes of GNP100–GNP50 possessed an LOD as low as 0.005 IU/ml (0.1 pM), which is 80 times more sensitive than ELISA and doubly more sensitive than our localized SPR property-based immunoassay biosensor using the same antigen–antibody pair [19]. This high sensitivity should owe to the detection model using two nanoprobes simultaneously, in which the signal was dually amplified during detection. Likewise, if the HBsAg molecule was captured by only one of the nanoprobes, the particle size of the nanoprobe would also be increased because the DLS technique was more sensitive than TEM and atomic force microscopy in reflecting exactly the interactions of flexible shell and metallic substrate.

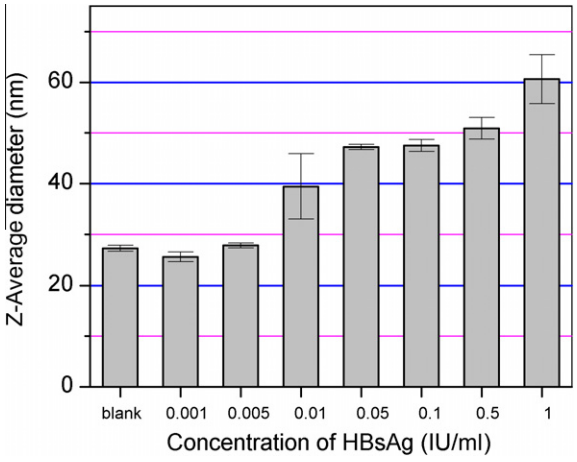

Fig.3. *Z*-Average diameters of the combination GNP10–GNP50 on the addition of HBsAg standard materials in Tris–HCl buffer.

It is important to note that in this experiment, there was no linear relationship between *Z*-average diameters and the concentrations, probably due to the fact that after aggregates were formed the particles or clusters measured as a unit by DLS were far from sphere shaped, as illustrated in Fig. 2. This would have a nonlinear influence on the rate of the particle's motion under Brownian diffusion. Furthermore, inspection of the micrographs displayed in Fig. 5A (before) and B (after) reveals that after the target was added, the dispersion state of the mixed nanoprobes changed remarkably. The detection system of GNP10–GNP50 was taken as an example because it was easier to distinguish between these two nanoparticles through TEM. As shown in Fig. 5A, only a few clusters of GNP10 nanoprobes had a relationship with those of GNP50s in the field of vision before detection. However, distinct interactions between the two kinds of nanoprobes are visually presented in Fig. 5B1 and B2 in the presence of the target. Meanwhile, it was observed that the GNP10s aggregated with each other in some microregions (Fig. 5B3). In our opinion, this phenomenon is a consequence of the aggregates described in Fig. 2Bb, where the analyte served as a bridge to link the GNP10s because of the polyclonal nature of GNP10s.

Detecting HBsAg in serum media

After the optimized combination was identified, we proceeded to investigate the applications of the current strategy in analyzing HBsAg in HBV-infected serum. To our knowledge, most of the newly developed nanoparticle-based immunoassays are not suited to analyzing protein in complex biological media such as plasma, serum, urine, and other biological fluids. A few researchers have focused their work on analyzing desired protein in actual media [19,44–46] because there are so many components in them, including dissolved protein, glucose, clotting factors, and hormones, which would disturb the stability of the nanoprobes or have great influence on their detection behavior. The biomacromolecules could also contribute to the intensity of light scattering. However, dark field imaging technology has demonstrated that in the same size domain, the serum particles have much weaker light scattering intensity than polystyrene latex particles and GNPs (http://www.nanodiscoveryinc.com). In this respect, it is theoretically feasible to use the as-prepared biosensor assay in the detection of HBsAg in actual serum. In fact, a series of recent studies has shown great promise that the DLS technique is capable of directly analyzing target analyte, even viruses, in complex biological media, such as tissue lysates, cell lysates, and blood serum [41,47–50]. The results of employing GNP50–GNP100 to analyze HBsAg in serum samples are illustrated in Fig. 6. The clinical samples were taken from infected human subjects whose serum had been determined by ELISA as infected or healthy. The shaded region corresponds to 3 times the standard deviation of the negative serum. As shown, the mixed nanoprobes were capable of distinguishing

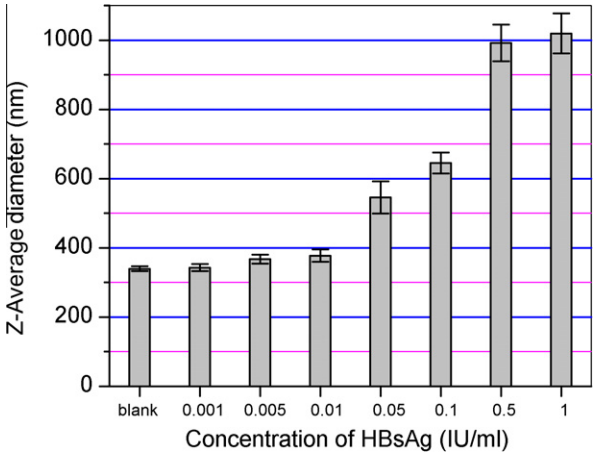

Fig.4. *Z*-Average diameters of the combination GNP100–GNP50 on the addition of HBsAg standard materials in Tris–HCl buffer.

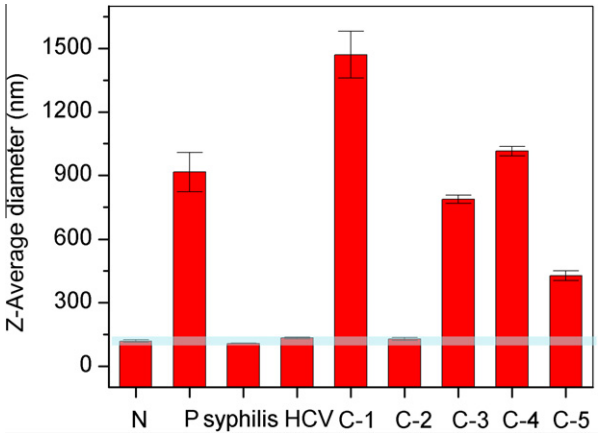

Fig.6. Applications of combination of GNP100–GNP50 to analyze HBsAg in serum samples. P: HBsAg-positive serum from commercial diagnostic kits; N: HBsAg-negative serum from commercial diagnostic kits; C-1, C-2, C-3, C-4, and C-5: Clinical samples taken from HBV-infected or healthy human subjects.

HBV-positive serum from HBV-negative serum as well as syphilis and HCV samples. In the case of the five clinical samples, the results of the current assay also matched well those of ELISA. Obviously, compared with the data of blank samples in Fig. 4, the particle sizes of the negative control samples in serum media decreased by more than 100 nm. Our interpretation is that the high content of blood protein, which was milligram grade, had dragged down the average particle size. For the purpose of clinical applications, the sample size of the background signal would be enlarged to increase the accuracy of the bioassay. However, compared with previous DLS-based biosensor assays, the current work has taken a step forward by using the light scattering property of GNPs in clinical diagnosis. Furthermore, the assay is straightforward in manipulation, including fabricating, labeling, and detection, which should open up new areas in using it in detection of other pathogens or biomarkers in actual media.

Conclusion

A homogeneous nanosensor assay has been designed to detect the biomarkers of HBV by target-induced aggregation monitored by DLS through the sandwich model. Three sorts of nanoprobes were prepared by labeling antibodies onto the surfaces of GNPs. The combinations of GNP10–GNP50 and GNP100–GNP50 were evaluated, and the latter was considered as the optimized one because of the much stronger DLS intensity of GNP100s in comparison with GNP10s. The mixed nanoprobes were demonstrated to be capable of capturing HBsAg target not only in Tris–HCl buffer but also in the serum media by measuring their hydrodynamic sizes. The *Z*-average diameters of the combination of GNP100–GNP50 increased in a dependent manner, with the concentrations of HBsAg ranging from 0.005 to 1 IU/ml. The nanoparticles and clusters observed by TEM visually confirmed that the size increase is indeed

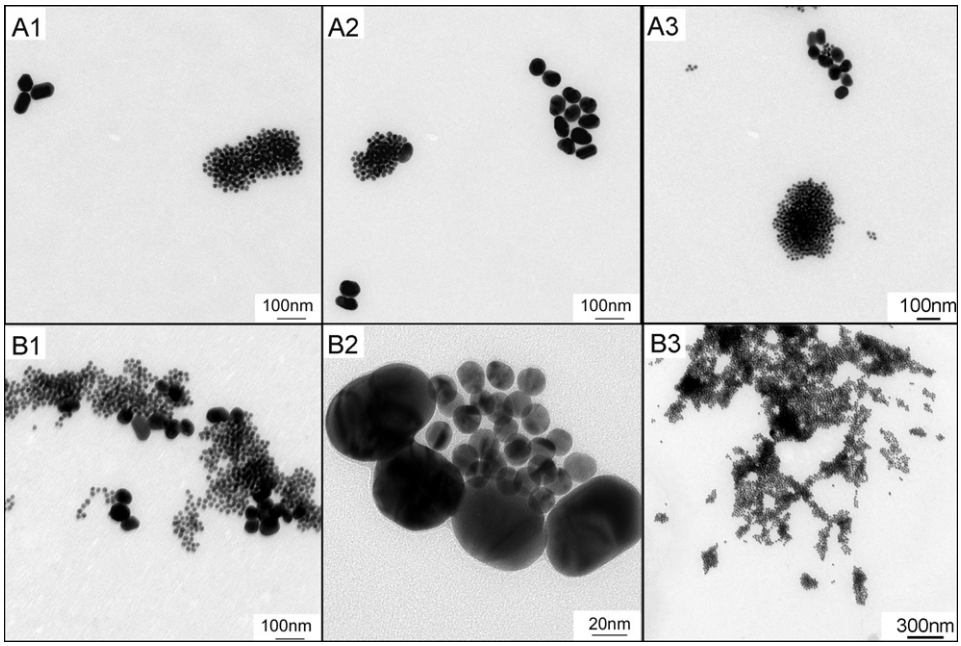

Fig.5. Representative TEM micrographs of the mixed nanoprobes of GNP10s and GNP50s. Panels A1 to A3 (top row): before detection. Panels B1 to B3: after 1 IU/ml HBsAg incubated with the mixed nanoprobes.

due to the aggregation caused by immunological reactions. Using the same antigen–antibody pair, this assay is 80 times more sensitive than the ELISA method under optimized conditions, which provides a useful means to analyze other protein biomarkers with low virus loads. Given the easy preparation of such nanoprobes, it is reasonable to believe that this light scattering-based immunoassay exhibits a good prospect of application in the future, and it can be developed into a common method to detect biomarkers in other actual media, such as plasma, saliva, and urine. It is believed that the DLS-based detection technology would also be developed into a powerful tool to shed light on the interactions among proteins, metal ions, and nucleic acids.

Acknowledgments

The authors thank Prof. Yiguang Jin and Dr. Miao Li in Beijing Institute of Radiation Medicine for their helpful discussions and technology support in characterizations. This work was supported by the Chinese National 863 Plan (2006AA03Z326) and the Beijing New Star Project on Science & Technology of China (2010B042).

References

[1] C.D. Medley, J.E. Smith, Z. Tang, Y. Wu, S. Bamrungsap, W. Tan, Gold nanoparticle-based colorimetric assay for the direct detection of cancerous cells, Anal. Chem. 80 (2008) 1067–1072.
[2] C. Yu, J. Irudayaraj, Multiplex biosensor using gold nanorods, Anal. Chem. 79 (2007) 572–579.
[3] C. Yu, J. Irudayaraj, Quantitative evaluation of sensitivity and selectivity of multiplex nanoSPR biosensor assays, Biophys. J. 93 (2007) 3684–3692.
[4] D.-Q. Feng, G. Liu, W. Zheng, J. Liu, T. Chen, D. Li, A highly selective and sensitive on–off sensor for silver ions and cysteine by light scattering technique of DNA-functionalized gold nanoparticles, Chem. Commun. 47 (2011) 8557–8559.
[5] M.A. Molina-Delgado, M.P. Aguilar–Caballos, A. Gómez-Hens, Usefulness of gold nanoparticles as labels for the determination of gliadins by immunoaffinity chromatography with light scattering detection, Talanta 85 (2011) 2391–2396.
[6] H. Jans, Q. Huo, Gold nanoparticle-enabled biological and chemical detection and analysis, Chem. Soc. Rev. 41 (2012) 2849–2866. and references cited therein.
[7] E. Boisselier, D. Astruc, Gold nanoparticles in nanomedicine: preparations imaging diagnostics therapies and toxicity, Chem. Soc. Rev. 38 (2009) 1759–1782. and references cited therein.
[8] J. Oishi, X. Han, J.-H. Kang, Y. Asami, T. Mori, T. Niidome, Y. Katayama, High-throughput colorimetric detection of tyrosine kinase inhibitors based on the aggregation of gold nanoparticles, Anal. Biochem. 373 (2008) 161–163.
[9] E.B. Dickerson, E.C. Dreaden, X. Huang, I.H. El-Sayed, H. Chu, S. Pushpanketh, J.F. McDonald, M.A. El-Sayed, Gold nanorod assisted near-infrared plasmonic photothermal therapy (PPTT) of squamous cell carcinoma in mice, Cancer Lett. 269 (2008) 57–66.
[10] P.-J. Debouttière, S. Roux, F. Vocanson, C. Billotey, O. Bæuf, A. Favre-Réguillon, Y. Lin, S. Pellet-Rostaing, R. Lamartine, P. Perriat, O. Tillement, Design of gold nanoparticles for magnetic resonance imaging, Adv. Funct. Mater. 16 (2006) 2330–2339.
[11] R.A. Sperling, P.R. Gil, F. Zhang, M. Zanella, W.J. Parak, Biological applications of gold nanoparticles, Chem. Soc. Rev. 37 (2008) 1896–1908.
[12] I.H. El-Sayed, X. Huang, M.A. El-Sayed, Selective laser photo-thermal therapy of epithelial carcinoma using anti-EGFR antibody conjugated gold nanoparticles, Cancer Lett. 239 (2006) 129–135.
[13] C. Wang, J. Chen, T. Talavage, J. Irudayaraj, Gold nanorods/Fe_3O_4 nanoparticle "nano-pearl-necklaces" for simultaneous targeting, dual-mode imaging, and photothermal ablation of cancer cells, Angew. Chem. Int. Ed. 121 (2009) 2797–2801.
[14] R.S. Norman, J.W. Stone, A. Gole, C.J. Murphy, T.L. Sabo-Attwood, Targeted photothermal lysis of the pathogenic bacteria, *Pseudomonas aeruginosa*, with gold nanorods, Nano Lett. 8 (2008) 302–306.
[15] A.M. Alkilany, L.B. Thompson, S.N. Boulos, P.N. Sisco, C.J. Murphy, Gold nanorods: their potential for photothermal therapeutics and drug delivery, tempered by the complexity of their biological interactions, Adv. Drug Deliv. Rev. 64 (2012) 190–199. and references cited therein.
[16] J.R. Kalluri, T. Arbneshi, S.A. Khan, A. Neely, P. Candice, B. Varisli, M. Washington, S. McAfee, B. Robinson, S. Banerjee, A.K. Singh, D. Senapati, P.C. Ray, Use of gold nanoparticles in a simple colorimetric and ultrasensitive dynamic light scattering assay: selective detection of arsenic in groundwater, Angew. Chem. Int. Ed. 121 (2009) 9848–9851.
[17] X. Yang, H. Liu, J. Xu, X. Tang, H. Huang, D. Tian, A simple and cost-effective sensing strategy of mercury(II) based on analyte-inhibited aggregation of gold nanoparticles, Nanotechnology 22 (2011) 275503.
[18] Y. Guo, Z. Wang, W. Qu, H. Shao, X. Jiang, Colorimetric detection of mercury, lead, and copper ions simultaneously using protein-functionalized gold nanoparticles, Biosens. Bioelectron. 26 (2011) 4064–4069.
[19] X. Wang, Y. Li, H. Wang, Q. Fu, J. Peng, Y. Wang, J. Du, Y. Zhou, L. Zhan, Gold nanorod-based localized surface plasmon resonance biosensor for sensitive detection of hepatitis B virus in buffer, blood serum, and plasma, Biosens. Bioelectron. 26 (2010) 404–410.
[20] K.M. Mayer, S. Lee, H. Liao, B.C. Rostro, A. Fuentes, P.T. Scully, C.L. Nehl, J.H. Hafner, A label-free immunoassay based upon localized surface plasmon resonance of gold nanorods, ACS Nano 2 (2008) 687–692.
[21] H. He, C. Xie, J. Ren, Nonbleaching fluorescence of gold nanoparticles and its applications in cancer cell imaging, Anal. Chem. 80 (2008) 5951–5957.
[22] C.C. You, O.R. Miranda, B. Gider, P.S. Ghosh, I.B. Kim, B. Erdogan, S.A. Krovi, U.H.F. Bunz, V.M. Rotello, Detection and identification of proteins using nanoparticle–fluorescent polymer "chemical nose" sensors, Nat. Nanotechnol. 2 (2007) 318–323.
[23] S. Lee, E.J. Cha, K. Park, S.Y. Lee, J.K. Hong, I.C. Sun, S.Y. Kim, K. Choi, I.C. Kwon, K. Kimand, C.H. Ahn, A near-infrared fluorescence-quenched gold nanoparticle imaging probe for in vivo drug screening and protease activity determination, Angew. Chem. Int. Ed. 120 (2008) 2846–2849.
[24] J.M. Nam, C.S. Thaxton, C.A. Mirkin, Nanoparticle-based bio-bar codes for the ultrasensitive detection of protein, Science 301 (2003) 1884–1886.
[25] Y.P. Bao, T.P. Wei, P.A. Lefebvre, H. An, L. He, G.T. Kunkeland, U.R. Müller, Detection of protein analytes via nanoparticle-based bio bar code technology, Anal. Chem. 78 (2006) 2055–2059.
[26] D.G. Georganopoulou, L. Chang, J.M. Nam, C.S. Thaxton, E.J. Mufson, W.L. Kleinand, C.A. Mirkin, Nanoparticle-based detection in cerebral spinal fluid of a soluble pathogenic biomarker for Alzheimer's disease, Proc. Natl. Acad. Sci. USA 102 (2005) 2273–2276.
[27] S.I. Stoeva, J.S. Lee, J.E. Smith, S.T. Rosenand, C.A. Mirkin, Multiplexed detection of protein cancer markers with biobarcoded nanoparticle probes, J. Am. Chem. Soc. 128 (2006) 8378–8379.
[28] E.D. Goluch, J.M. Nam, D.G. Georganopoulou, T.N. Chiesl, K.A. Shaikh, K.S. Ryu, A.E. Barron, C.A. Mirkin, C. Liu, A bio-barcode assay for on-chip attomolar-sensitivity protein detection, Lab. Chip 6 (2006) 1293–1299.
[29] S. Tang, J. Zhao, J.J. Storhoff, P.J. Norris, R.F. Little, R. Yarchoan, S.L. Stramer, T. Patno, M. Domanus, A. Dhar, C.A. Mirkin, I.K. Hewlett, Nanoparticle-based biobarcode amplification assay (BCA) for sensitive and early detection of human immunodeficiency type 1 capsid (p24) antigen, J. AIDS 46 (2007) 231–237.
[30] H. Huang, C. Tang, Y. Zeng, X. Yu, B. Liao, X. Xia, P. Yi, P.K. Chu, Label-free optical biosensor based on localized surface plasmon resonance of immobilized gold nanorods, Colloids Surf. B 71 (2009) 96–101.
[31] R.J. Cohen, G.B. Benedek, Laser light scattering spectroscopic immunoassay in the agglutination inhibition mode for human chorionic gonadotropin, HCG) and human luteinizing hormone (hLH), Immunochemistry 12 (1975) 963–966.
[32] H. Jans, X. Liu, L. Austin, G. Maes, Q. Huo, Dynamic light scattering as a powerful tool for gold nanoparticle bioconjugation and biomolecular binding studies, Anal. Chem. 81 (2009) 9425–9432.
[33] L. Austin, X. Liu, Q. Huo, Gold nanoparticle probes coupled with dynamic light scattering for monoclonal antibody analysis and binding study, Am. Biotechnol. Lab. 28 (2010) 8–12.
[34] X.M. Miao, C. Xiong, W.W. Wang, L.S. Liang, X.T. Shuai, Dynamic-light-scattering-based sequence-specific recognition of double-stranded DNA with oligonucleotide-functionalized gold nanoparticles, Chem. Eur. J. 17 (2011) 11230–11236.
[35] Q. Dai, X. Liu, J. Coutts, L. Austin, Q. Huo, A one-step highly sensitive method for DNA detection using dynamic light scattering, J. Am. Chem. Soc. 130 (2008) 8138–8139.
[36] X. Liu, Q. Dai, L. Austin, J. Coutts, G. Knowles, J. Zou, H. Chen, Q. Huo, A one-step homogeneous immunoassay for cancer biomarker detection using gold nanoparticle probes coupled with dynamic light scattering, J. Am. Chem. Soc. 130 (2008) 2780–2782.
[37] P.K. Jain, K.S. Lee, I.H. El-Sayed, M.A. El-Sayed, Calculated absorption and scattering properties of gold nanoparticles of different size, shape, and composition: Applications in biological imaging and biomedicine, J. Phys. Chem. B 110 (2006) 7238–7248.
[38] G. Frens, Controlled nucleation for the regulation of the particle size in monodisperse gold suspensions, Nat. Phys. Sci. 241 (1973) 20–22.
[39] M. Horisberger, J. Rosset, Colloidal gold, a useful marker for transmission and scanning electron microscopy, J. Histochem. Cytochem. 25 (1977) 295–305.
[40] J. Peng, X. Liu, X. Ding, Z. Fu, Q. Wang, Evaluation of the particle diameter of colloidal gold and its distribution through visible spectroscopy, Bull. Acad. Mil. Med. Sci. 24 (2000) 211–212.
[41] J.D. Driskell, C.A. Jones, S.M. Tomkins, R.A. Tripp, One-step assay for detecting influenza virus using dynamic light scattering and gold nanoparticles, Analyst 136 (2011) 3083–3090.
[42] W. Haiss, N.T.K. Thanh, J. Aveyard, D.G. Fernig, Determination of size and concentration of gold nanoparticles from UV–Vis spectra, Anal. Chem. 79 (2007) 4215–4221.
[43] X. Liu, Q. Huo, A washing-free and amplification-free one-step homogeneous assay for protein detection using gold nanoparticle probes and dynamic light scattering, J. Immunol. Methods 349 (2009) 38–44.
[44] S.J. Osterfeld, H. Yu, R.S. Gaster, S. Caramuta, L. Xu, S.J. Han, D.A. Hall, R.J. Wilson, S. Sun, R.L. White, R.W. Davis, N. Pourmand, S.X. Wang, Multiplex

protein assays based on real-time magnetic nanotag sensing, Proc. Natl. Acad. Sci. USA 105 (2008) 20637–20640.
[45] X. Xia, Y. Xu, X. Zhao, Q. Li, Lateral flow immunoassay using europium chelate-loaded silica nanoparticles as labels, Clin. Chem. 55 (2009) 179–182.
[46] R.S. Gaster, D.A. Hall, C.H. Nielsen, S.J. Osterfeld, H. Yu, K.E. Mach, R.J. Wilson, B. Murmann, J.C. Liao, S.S. Gambhir, S.X. Wang, Matrix-insensitive protein assays push the limits of biosensors in medicine, Nat. Med. 15 (2009) 1327–1332.
[47] Q. Huo, Protein complexes/aggregates as potential cancer biomarkers revealed by a nanoparticle aggregation immunoassay, Colloids Surf. B 78 (2010) 259–265.
[48] Q. Huo, J. Colon, A. Cordero, J. Bogdanovic, C.H. Baker, S. Goodison, M.Y. Pensky, A facile nanoparticle immunoassay for cancer biomarker discovery, J. Nanobiotechnol. 9 (2011) 1–12.
[49] Q. Huo, S.A. Litherland, S. Sullivan, H. Hallquist, D.A. Decker, I. Rivera-Ramirez, Developing a nanoparticle test for prostate cancer scoring, J. Transl. Med. (2012), http://dx.doi.org/10.1186/1479-5876-10-44.
[50] S. Jaganathan, P. Yue, D.C. Paladino, J. Bogdanovic, Q. Huo, J. Turkson, A functional nuclear epidermal growth factor receptor: Src and Stat3 heteromeric complex in pancreatic cancer cells, PLoS One 6 (2011) e19605.